

Universality in the three-body problem for ^4He atoms

Eric Braaten* and H.-W. Hammer†

Department of Physics, The Ohio State University, Columbus, Ohio 43210

(Received 22 March 2002; published 11 April 2003)

The two-body scattering length a for ^4He atoms is much larger than their effective range r_s . As a consequence, low-energy few-body observables have universal characteristics that are independent of the interaction potential. Universality implies that, up to corrections suppressed by r_s/a , all low-energy three-body observables are determined by a and a three-body parameter Λ_* . We give simple expressions in terms of a and Λ_* for the trimer binding-energy equation, the atom-dimer scattering phase shifts, and the rate for three-body recombination at threshold. We determine Λ_* for several ^4He potentials from the calculated binding energy of the excited state of the trimer and use it to obtain the universality predictions for the other low-energy observables. We also use the calculated values for one potential to estimate the effective range corrections for the other potentials.

DOI: 10.1103/PhysRevA.67.042706

PACS number(s): 03.65.Nk, 36.40.-c, 21.45.+v, 03.65.Ge

I. INTRODUCTION

The interactions of nonrelativistic particles with extremely low energies, such as cold atoms, are determined primarily by their S -wave scattering length a . Typically, $|a|$ is of the order of the natural length scale l associated with low-energy interactions, which for short-range interactions is given by the range of the potential. If $|a|$ is much larger than l , however, low-energy atoms exhibit universal properties that are independent of the interaction potential. In the two-body sector, universality implies that low-energy observables are determined by the single parameter a up to corrections suppressed by $l/|a|$. In particular, the cross section for low-energy atom-atom scattering is a simple function of E and a only. If $a > 0$, there is also a shallow two-body bound state (the dimer) whose binding energy is determined by a : $B_2 = \hbar^2/ma^2$, where m is the mass of the atoms [1].

Efimov showed that if the two-body scattering length is large, there are also universal properties in the three-body sector [2]. The most remarkable is a sequence of three-body bound states (trimers) with binding energies geometrically spaced in the interval between \hbar^2/ma^2 and \hbar^2/ml^2 . In addition to the binding energies of these Efimov trimers, the low-energy three-body observables include scattering rates for three atoms and, if $a > 0$, an atom and a dimer. The consequences of universality in the three-body sector are simplest if the potential supports no deep two-body bound states with binding energies of order \hbar^2/ml^2 . In this case, the low-energy three-body observables are determined by a and a single three-body parameter up to corrections suppressed by $l/|a|$. A simple physical observable that can be used as the three-body parameter is the binding energy of the Efimov state closest to threshold. Alternatively, the three-body parameter can be specified by a boundary condition on the three-body wave function at short distances. In Ref. [3], the authors introduced a more abstract three-body parameter Λ_*

with dimensions of wave number [defined in Eq. (10) below], which is particularly convenient for quantitative calculations within the effective field theory approach.

A large two-body scattering length can be obtained by fine tuning a parameter in the interatomic potential to bring a real or virtual two-body bound state close to the two-atom threshold. The fine tuning can be obtained experimentally by adjusting an external variable, such as a magnetic field [4] or an electric field [5]. Large scattering lengths for ^{23}Na and ^{85}Rb atoms have been obtained in the laboratory by tuning an external magnetic field to the neighborhood of a Feshbach resonance [6]. The fine tuning can also be provided accidentally by nature. A prime example is the ^4He atom, whose scattering length $a \approx 104 \text{ \AA}$ [7] is much larger than its effective range $r_s \approx 7.3 \text{ \AA}$ [8], which can be taken as an estimate of the natural low-energy length scale l .

The large scattering length for ^4He makes this atom an ideal example of universality. The experimental information on low-energy ^4He atoms is rather limited. Using diffraction of a molecular beam of small ^4He clusters from a transmission grating, the bond length of the ^4He dimer has recently been measured [7]: $\langle r \rangle = (52 \pm 4) \text{ \AA}$, which is an order of magnitude larger than the effective range. The scattering length $a = 104_{-18}^{+8} \text{ \AA}$ and the dimer binding energy $B_2 = 1.1_{-0.2}^{+0.3} \text{ mK}$ were derived from the measured bond length using the zero-range approximation [7]. The ^4He trimer and several larger ^4He clusters have been observed [9,10], but no quantitative experimental information about their binding energies is available to date. However, there have been extensive theoretical calculations of the few-body problem for ^4He using modern two-body potentials [11,12]. Theoretical calculations of trimer binding energies have also improved, so that they now have several digits of accuracy [13–16]. They indicate that there are two trimers: a ground state with binding energy $B_3^{(0)}$ and an excited state with binding energy $B_3^{(1)}$. The ground-state binding energies of larger ^4He clusters have been calculated using the diffusion Monte Carlo method [16]. Their excited-state binding energies have been calculated using a combination of Monte Carlo methods and the hyperspherical adiabatic approximation [17]. There have also been some calculations on three-body scattering observ-

*Electronic address: braaten@mps.ohio-state.edu

†Present address: Helmholtz-Institut für Strahlen- und Kernphysik (Theorie), Universität Bonn, Nussallee 14-16, 53115 Bonn, Germany. Electronic address: hammer@itkp.uni-bonn.de

ables. The S -wave phase shifts for atom-dimer scattering have been calculated in Refs. [3,15]. The three-body recombination rate has been calculated at threshold [18–21] and as a function of energy [22].

Universality implies that in the limit of large scattering length, all low-energy three-body observables are determined by the scattering length a (or equivalently the dimer binding energy B_2) and one three-body parameter such as Λ_* . In order to determine this parameter, a low-energy three-body observable is required as input. We can take advantage of the accurate calculations of the trimer binding energies for modern ^4He potentials by using $B_3^{(1)}$ to determine Λ_* for ^4He . Once this parameter is determined, universality can be used to predict all other low-energy three-body observables for ^4He atoms.

We can also exploit accurate theoretical calculations for older ^4He potentials to demonstrate the nontrivial nature of universality in the three-body sector [23,24]. Scaling variables are dimensionless combinations of physical observables. Universality implies that three-body scaling variables are nontrivial universal functions of $a\Lambda_*$. By eliminating the dependence on Λ_* , we can express one scaling variable as a universal function of any other scaling variable. The various ^4He potentials have slightly different scattering lengths a and also different values of Λ_* . Therefore, if one scaling variable is plotted as a function of a second, the points for various ^4He potentials should all lie along a universal line. Frederico, Tomio, Delfino, and Amorim calculated the scaling function relating $B_3^{(1)}/B_3^{(0)}$ to $B_2/B_3^{(0)}$ and showed that the points for various ^4He potentials lie close to the universal scaling curve [23,24].

In this paper, we collect all the information that is currently available on the universal properties in the three-body system of ^4He atoms. We go beyond the work in Refs. [23,24] in various respects. We give explicit parametrizations in terms of a and the three-body parameter Λ_* for many low-energy three-body observables, including Efimov binding energies, atom-dimer scattering phase shifts, and the three-body recombination rate. We also calculate additional scaling functions and estimate the effective range corrections. In Sec. II, we briefly review universality in the two-body sector. In Sec. III, we discuss the universal properties of the trimer binding energies. We determine the three-body parameter Λ_* for various ^4He potentials from the excited state binding energy $B_3^{(1)}$ and use universality to predict the ground-state energy $B_3^{(0)}$. We also demonstrate universality by exhibiting the correlation between the scaling variables $B_3^{(0)}/B_2$ and $B_3^{(1)}/B_2$ for various ^4He potentials. In Secs. IV and V, we discuss the universal properties in atom-dimer scattering and three-body recombination, respectively. We use universality to predict the S -wave scattering length a_{12} and effective range $r_{s,12}$ for atom-dimer scattering as well as the rate constant for three-body recombination at threshold. We also demonstrate universality by exhibiting the correlations between the scaling variable a_{12}/a and the energy scaling variables for various ^4He potentials. Section VI contains a summary and the outlook for using universality as the basis for a quantitative description of cold atoms.

II. TWO-BODY SECTOR

We begin by reviewing the universal properties in the two-body sector for ^4He [1]. We use the phrase “low-energy” to refer to energies close to the threshold for free atoms. There is a natural length scale l for low-energy observables. For a short-range potential, l is set by the range. If the potential has a van der Waals tail, $V(r) \rightarrow -C_6/r^6$, the natural low-energy length scale is $l \approx (mC_6/\hbar^2)^{1/4}$. The natural energy scale for low-energy observables is \hbar^2/ml^2 . For ^4He , $C_6 = 1.46$ a.u. which leads to $l = 5$ Å and $\hbar^2/ml^2 = 0.4$ K. Universality occurs because a parameter in the two-body potential has been tuned such that the scattering length is unnaturally large. The scattering length $a = 104$ Å [7] for ^4He is much larger than l . We can interpret the large scattering length as the result of an accidental fine tuning by nature of either a parameter in the two-body potential, such as its overall strength, or of the mass of the ^4He atom. The ^3He atom has a mass that is only about 3/4 of that of ^4He , and its scattering length is -7.1 Å [11], close in magnitude to the natural low-energy length scale.

If $|a| \gg l$, universality can be used to describe the low-energy observables for atoms in spite of the fact that the van der Waals tail makes the potential long range. Explicit expressions for the scattering length and effective range for a potential with a van der Waals tail have been derived in Ref. [25]. A long-range potential introduces nonanalytic behavior in the dependence of the scattering amplitudes on the wave vector \mathbf{k} . However if the potential falls off like $1/r^6$, this nonanalytic behavior enters first at fourth order in k . Such effects cannot be reproduced by a short-range potential. Fortunately, their effects on low-energy observables are suppressed by four powers of l/a . We will focus on the universality predictions at leading order in l/a and also on the effective range corrections that are first order in l/a . At this level of accuracy, the effects of the van der Waals tail on low-energy observables can be reproduced by a short-range potential. Realistic interatomic potentials will therefore exhibit the same universal characteristics as short-range potentials.

The two-body observables are the differential cross sections for two-body scattering and the binding energies for two-body bound states. The differential cross section for the elastic scattering of two identical spinless bosons with total energy $E = \hbar^2 k^2/m$ has the general form

$$\frac{d\sigma}{d\Omega} = 4 \left| \sum_{L \text{ even}} \frac{2L+1}{k \cot \delta_L(k) - ik} P_L(\cos \theta) \right|^2, \quad (1)$$

where $\delta_L(k)$ is the phase shift for the L th partial wave. The total cross section is obtained from Eq. (1) by integrating over a solid angle of 2π to avoid counting identical particles twice. At low energies, the cross section is dominated by the $L=0$ “ S -wave” term. The effective range expansion of $k \cot \delta_0(k)$ has the form

$$k \cot \delta_0(k) = -\frac{1}{a} + \frac{1}{2} r_s k^2 + \dots \quad (2)$$

The first two coefficients define the scattering length a and the effective range r_s . The natural size for these coefficients is the low-energy length scale l . The binding energies of the two-body bound states are determined by the poles of the scattering amplitude. For S -wave bound states, the binding energies are $B_2^{(n)} = \hbar^2 \kappa_n^2 / m$, where κ_n is a solution to the equation

$$i\kappa \cot \delta_0(i\kappa) + \kappa = 0. \quad (3)$$

The natural energy scale for a bound state close to threshold is \hbar^2/ml^2 .

If the scattering length a is unnaturally large, the differential cross section exhibits universal behavior at energies small compared to \hbar^2/ml^2 :

$$\frac{d\sigma}{d\Omega} = \frac{4a^2}{1+k^2a^2}, \quad kl \ll 1, |a| \gg l. \quad (4)$$

The leading correction comes from the effective range. At wave number k of order $(r_s a)^{-1/2}$ or smaller, the error is of order r_s/a . At larger wave numbers, the error increases like $k^2 r_s^2$ and becomes of order one at k of order $1/r_s$. Note that the differential cross section (4) is determined as a function of k by the single parameter a .

If a is large and positive, there is one additional low-energy observable. There is a shallow two-body S -wave bound state that we will refer to as ‘‘the dimer.’’ Up to corrections suppressed by l/a , its binding energy is

$$B_2 = \frac{\hbar^2}{ma^2}, \quad a \gg l. \quad (5)$$

Alternatively, if we take B_2 as input, universality gives a prediction for the scattering length:

$$a_B \equiv \frac{\hbar}{\sqrt{mB_2}}. \quad (6)$$

The leading correction to the universal prediction for B_2 in Eq. (5) comes from the effective range. If we truncate the effective range expansion (2) after the k^2 term, Eq. (3) is a quadratic equation with two solutions,

$$B_2^{(\pm)} = \frac{\hbar^2}{m} \frac{2}{r_s^2} \left[1 - \frac{r_s}{a} \pm \sqrt{1 - 2\frac{r_s}{a}} \right]. \quad (7)$$

The solution $B_2^{(+)}$ is an artifact of the truncation. We would expect a state with such an energy only if the higher-order terms in the effective range expansion are unnaturally small. The solution $B_2^{(-)}$ is the binding energy of the shallow dimer. If we expand to first order in r_s/a , we obtain

$$B_2^{(-)} = \frac{\hbar^2}{ma^2} \left[1 + \frac{r_s}{a} \right]. \quad (8)$$

TABLE I. Two-body observables for four ${}^4\text{He}$ potentials. Lengths and energies are given in \AA and mK, respectively. The first three columns show the calculated scattering lengths a [15], effective ranges r_s [8], and dimer binding energies B_2 [15]. The last three columns show the universality predictions a_B for a using B_2 as input, the universality predictions for B_2 using a as input, and the predictions for B_2 including the first-order effective range correction. (For ${}^4\text{He}$, the conversion constant is $\hbar^2/m = 12.1194 \text{ K \AA}^2$.)

Potential	a	r_s	B_2	a_B	$\frac{\hbar^2}{ma^2}$	$B_2^{(-)}$
HFDHE2	124.65	7.396	0.83012	120.83	0.7800	0.8263
HFD-B	88.50	7.277	1.68541	84.80	1.5474	1.6746
LM2M2	100.23	7.326	1.30348	96.43	1.2064	1.2946
TTY	100.01	7.329	1.30962	96.20	1.2117	1.3005

The corrections from higher orders in the effective range expansion (2) are suppressed by l^2/a^2 and should therefore be comparable in magnitude to the r_s^2/a^2 correction.

We now consider the two-body observables for ${}^4\text{He}$. In Table I, we give the calculated scattering length [15], the effective range [8], and the dimer binding energies [15] for four commonly used potentials: two modern potentials LM2M2 [11] and TTY [12], and two older potentials HFDHE2 [26] and HFD-B [27].

In Table I, we also give some simple theoretical predictions for two-body observables. We give the prediction a_B for the scattering length obtained from Eq. (6) by using B_2 as input. We also give two predictions for the dimer binding energy B_2 using the scattering data a and r_s as input. They are the universality prediction in Eq. (5) and the prediction including the first-order effective range correction in Eq. (8). We can obtain estimates of the theoretical errors in approaches based on the universality at large a by comparing those approximations with the calculated value of B_2 . The universality prediction \hbar^2/ma^2 differs from B_2 by at most 8% and the errors decrease to at most 0.7% if the first-order effective range correction is included. This suggests that predictions of low-energy observables based on universality should have an accuracy of about 10% and that that one may be able to reduce the errors to about 1% by including effective range corrections.

III. TRIMER BINDING ENERGIES

The most dramatic prediction of universality in the three-body sector with large scattering length is the existence of Efimov states [2]. They are a sequence of shallow three-body bound states with binding energies much smaller than \hbar^2/ml^2 . If a parameter in the two-body potential is tuned such that $a \rightarrow \pm\infty$, the number of these states increases roughly as $\ln(|a|/l)/\pi$. The spacing of the deeper states is roughly geometric with the ratio of successive binding energies approaching 515. The suggestion that the excited state of the ${}^4\text{He}$ trimer is an Efimov state was first made in Ref. [28]. Accurate calculations using modern potentials support that interpretation [13–15,29]. In Refs. [3,23,30], it was ar-

gued that the trimer ground state is also an Efimov state. If it is an Efimov state, universality can be used to predict its binding energy. We will show that the resulting predictions are within the errors expected from effective range corrections. We will also give a definitive criterion for a three-body bound state to be an Efimov state.

Efimov derived some powerful constraints on low-energy three-body observables for systems with large scattering length [2]. They follow from the approximate scale invariance at length scales R in the region $l \ll R \ll |a|$ together with the conservation of probability. He introduced polar variables H and ξ in the plane whose axes are $1/a$ and the energy variable $\text{sgn}(E)|mE|^{1/2}/\hbar$. The angular variable ξ is

$$\xi = \begin{cases} -\arctan(a\sqrt{mB_3}/\hbar), & a > 0 \\ -\pi + \arctan(|a|\sqrt{mB_3}/\hbar), & a < 0. \end{cases} \quad (9)$$

Efimov showed that low-energy three-body observables are determined by a few universal functions of the angle ξ . In particular, the binding energies of the Efimov states are solutions to an equation involving a single universal function $\Delta(\xi)$ [2]. Efimov's equation for the binding energies reads [2,30]

$$B_3 + \frac{\hbar^2}{ma^2} = \frac{\hbar^2 \Lambda_*^2}{m} e^{2\pi n/s_0} \exp[\Delta(\xi)/s_0], \quad (10)$$

where $s_0 \approx 1.00624$ is a transcendental number that satisfies the equation

$$\sqrt{3} s_0 \cosh(\pi s_0/2) = 8 \sinh(\pi s_0/6). \quad (11)$$

We use a three-body parameter Λ_* that was first introduced in Ref. [3] through a rather technical definition specific to an effective-field theory. Efimov's Eq. (10), together with the explicit parametrization of $\Delta(\xi)$ given below in Eqs. (12)–(14) provides an equivalent definition of Λ_* . Note that we measure B_3 from the three-atom threshold, so $B_3 > B_2$ for $a > 0$. If the universal function $\Delta(\xi)$ is known, the Efimov binding energies B_3 can be calculated as a function of a and Λ_* by solving Eq. (10) for different values of the integer n . Equation (10) has an exact discrete scaling symmetry: if there is an Efimov state with binding energy B_3 for the parameters a and Λ_* , then there is also an Efimov state with binding energy $\lambda^2 B_3$ for the parameters $\lambda^{-1}a$ and Λ_* if $\lambda = \exp[n'\pi/s_0]$ with n' an integer. Due to this symmetry, Eq. (10) defines Λ_* only up to multiplicative factors of $\exp[\pi/s_0]$. If $a > 0$, the scattering length a in Eqs. (9) and (10) can be replaced by a_B defined in Eq. (6). The change in the predictions for B_3 when a_B is used instead of a can be taken as an estimate of the theoretical error associated with effective range corrections.

The universal function $\Delta(\xi)$ could be determined by solving the three-body Schrödinger equation for the Efimov binding energies in various potentials whose scattering lengths are so large that effective range corrections are negligible. It can be calculated more easily by using the effective field theory of Ref. [3] in which the effective range can be set to zero. In Ref. [3], the dependence of the binding

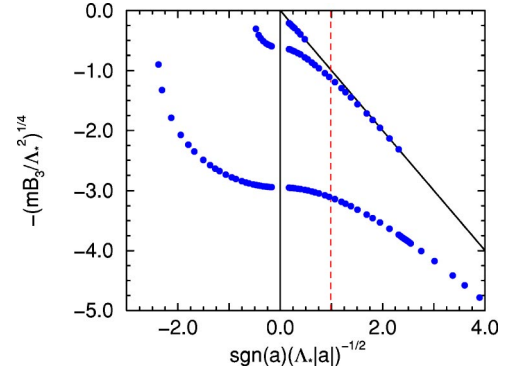


FIG. 1. The energy variable $-(mB_3/\hbar^2\Lambda_*^2)^{1/4}$ for three shallow Efimov states as a function of $\text{sgn}(a)(\Lambda_*|a|)^{-1/2}$. The vertical dashed line corresponds to the LM2M2 and TTY potentials for ^4He .

energy on a and Λ_* was calculated for the shallowest Efimov state and $a > 0$. In Ref. [30], the binding energies of the three lowest Efimov states were calculated for both signs of a and used to extract the universal function $\Delta(\xi)$. In Fig. 1, we plot $-(mB_3/\hbar^2\Lambda_*^2)^{1/4}$ as a function of $\text{sgn}(a)(\Lambda_*|a|)^{-1/2}$ for these three branches of Efimov states. The binding energies for deeper Efimov states and for shallower states near $(\Lambda_*|a|)^{-1/2} = 0$ can be obtained from the discrete scaling symmetry. Parametrizations of $\Delta(\xi)$ in various regions for ξ were obtained by fitting the Efimov spectrum [30],

$$\xi \in \left[-\frac{3\pi}{8}, -\frac{\pi}{4} \right]: \Delta = 3.10x^2 - 9.63x - 2.18, \quad (12)$$

$$x = (-\pi/4 - \xi)^{1/2},$$

$$\xi \in \left[-\frac{5\pi}{8}, -\frac{3\pi}{8} \right]: \Delta = 1.17y^3 + 1.97y^2 + 2.12y - 8.22, \quad (13)$$

$$y = \pi/2 + \xi,$$

$$\xi \in \left[-\pi, -\frac{5\pi}{8} \right]: \Delta = 0.25z^2 + 0.28z - 9.11, \quad (14)$$

$$z = (\pi + \xi)^2 \exp[-1/(\pi + \xi)^2].$$

These parametrizations deviate from the numerical results by less than 0.013. The discontinuity at $\xi = -3\pi/8$ and $\xi = -5\pi/8$ is less than 0.016. Using Eq. (10) and the parametrizations (12–14), the full spectrum of Efimov states can be calculated as a function of a and Λ_* . Equation (10) can also be used as an operational definition of the three-body parameter Λ_* , which was originally defined in the framework of effective field theory [3]. If the binding energy B_3 of an Efimov state is known either from experiment or by solving the three-body Schrödinger equation, we can determine Λ_* by demanding that B_3 be a solution to Eq. (10) for some integer n .

A given two-body potential is characterized by values of a and Λ_* and corresponds to a vertical line in Fig. 1. The

TABLE II. The trimer binding energies $B_3^{(0)}$ and $B_3^{(1)}$ in mK measured from the three-atom threshold for four ^4He potentials. The calculated values from Ref. [15] are in columns 1 and 2. The values of $a\Lambda_*$, the universality predictions for $B_3^{(0)}$, and the predictions for $B_3^{(0)}$ including effective range corrections using B_2 and $B_3^{(1)}$ as input are in columns 3–5. The corresponding values using a and $B_3^{(1)}$ as input are in columns 6–8. Numbers in brackets were used as input. LO and NLO represent leading order and next-to-leading order, respectively.

Potential	$B_3^{(0)}$	$B_3^{(1)}$	$a_B\Lambda_*$	$B_3^{(0)}$ (LO)	$B_3^{(0)}$ (NLO)	$a\Lambda_*$	$B_3^{(0)}$ (LO)	$B_3^{(0)}$ (NLO)
HFDHE2	116.7	1.67	1.258	118.5	116.7	1.364	129.1	119.3
HFD-B	132.5	2.74	0.922	137.5	[132.5]	1.051	159.7	[132.5]
LM2M2	125.9	2.28	1.033	130.3	126.8	1.155	147.4	128.6
TTY	125.8	2.28	1.025	129.1	125.6	1.147	146.4	127.5

dashed line shown corresponds to the LM2M2 and TTY potentials for ^4He atoms. The intersections of this line with the binding-energy curves correspond to the infinitely many Efimov states. The two intersections visible in the figure correspond to the excited state and the ground state of the ^4He trimer. The third bound state predicted by Efimov's equation has a binding energy that is $\approx 515B_3^{(0)} \approx 67$ K. This is much larger than the natural low-energy scale \hbar^2/ml^2 which is 0.4 K. This state and all the deeper Efimov states are therefore artifacts of the limit $a \gg l$.

We can use one of the trimer binding energies as the input to determine Λ_* . It is safer to use the binding energy $B_3^{(1)}$ of the excited state because it is least affected by the high-energy effects that cut off the Efimov spectrum. The most accurate calculations of $B_3^{(1)}$ have been obtained by solving the Faddeev equations in the hyperspherical representation [13], in configuration space [14], and with hard-core boundary conditions [15]. These methods give results that agree to within 0.6%. The results of Ref. [15] for $B_3^{(0)}$ and $B_3^{(1)}$ for the HFDHE2, HFD-B, LM2M2, and TTY potentials are given in Table II. The results for the binding energy $B_3^{(0)}$ of the ground state of the trimer agree well with diffusion Monte Carlo calculations [16], which give $B_3^{(0)} = (131.0 \pm 0.7)$ mK for the HFD-B potential and (125.5 ± 0.6) mK for the TTY potential. Taking the calculated dimer binding energy B_2 as the two-body input, we determine Λ_* by demanding that $B_3^{(1)}$ satisfy Eq. (10) with $n=1$. Solving Eq. (10) with $n=2$, we obtain the predictions for $B_3^{(0)}$ in column 4 of Table II. The predictions are only 1–4% higher than the calculated values. If we use the calculated values of a as input instead of B_2 , we obtain the predicted values of $B_3^{(0)}$ in column 7 of Table II. These values are larger than the calculated ones by 11–21%. The difference between these predictions and those obtained by using B_2 and $B_3^{(1)}$ as the input gives an indication of the size of effective range corrections. The predictions are labeled LO in Table II because they are the universality prediction at “leading order” in r_s/a .

The numerical values of Λ_* for the four potentials in the Table II are nearly the same. If we use a_B and $B_3^{(0)}$ as the input, we obtain $\Lambda_* = 0.0107 \text{ \AA}^{-1}$ for the LM2M2 and TTY potentials. The values for the other two potentials differ by less than 3%. If we use a and $B_3^{(0)}$ as the input, we obtain $\Lambda_* = 0.0115 \text{ \AA}^{-1}$ for the LM2M2 and TTY potentials. The values for the other two potentials differ by less than 5%.

The small differences between the values of Λ_* for these potentials illustrates the fact that Λ_* tends to be insensitive to the parameter in the potential that is tuned to make the scattering length large.

The availability of accurate calculations of $B_3^{(0)}$ and $B_3^{(1)}$ for various older ^4He potentials can be used to demonstrate the nontrivial nature of universality in the three-body sector. Different potentials that give a large two-body scattering length should correspond to different values of Λ_* . The scaling variables $B_3^{(0)}/B_2$ and $B_3^{(1)}/B_2$ are functions of $a\Lambda_*$ only. If we eliminate Λ_* , we obtain a prediction for $B_3^{(1)}/B_2$ as a universal function of $B_3^{(0)}/B_2$. A closely related scaling function that expresses $B_3^{(1)}/B_3^{(0)}$ as a function of $B_2/B_3^{(0)}$ has been calculated by Frederico, Tomio, Delfino, and Amorim using the renormalized zero-range model [23,24]. We have reproduced their scaling function using the solution to Efimov's equation (10). In Fig. 2, our calculation of the universal scaling function relating $B_3^{(1)}/B_2$ to $B_3^{(0)}/B_2$ is shown as a solid line. As Λ_* increases, one moves along the solid line to the right. The data points in Fig. 2 are the results from calculations with various ^4He potentials. The filled symbols show the results from Motovilov *et al.* [15], which we used to determine Λ_* for each potential, while the open symbols display the results from various other calculations

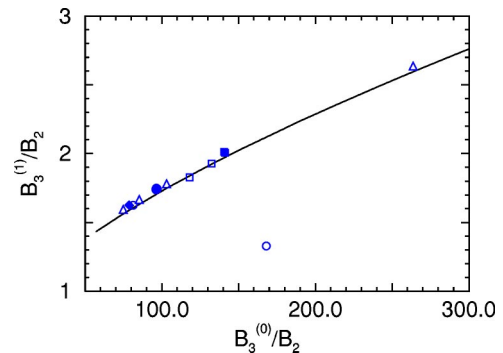


FIG. 2. The excited-state energy $B_3^{(1)}$ as a function of the ground-state energy $B_3^{(0)}$. The solid line is the universal scaling curve predicted by Eq. (10). The filled symbols show the results from Motovilov *et al.* [15], while the open symbols display the results from various other calculations [13,14,29,31,32]. The results for the LM2M2/TTY, HFDHE2, and HFD-B potentials are indicated by the circles, squares, and diamonds, respectively. The open triangles show results from Ref. [14] for four other potentials.

[13,14,29,31,32]. The results for the LM2M2/TTY, HFDHE2, and HFD-B potentials are displayed by the circles, squares, and diamonds, respectively. The open triangles show results from Ref. [14] for four other potentials.

The points fall very close to the universal scaling curve, with the exception of the result of Ref. [32] for the LM2M2 potential, which lies well below. In that paper, the overall strength of the potential was varied such that B_2 passed through zero. The results failed to exhibit the Efimov effect of an accumulation of three-body bound states at threshold as $B_2 \rightarrow \infty$. The numerical accuracy of this calculation has been questioned in Ref. [33]. All the remaining results fall along the universal scaling curve. This demonstrates that the dominant effect of the different potentials on the trimer binding energies can be described by a single parameter that we can identify with Λ_* .

It is interesting to note that calculations using only the lowest adiabatic hyperspherical potential [29] or the lowest orbital angular-momentum wave function give results that already lie near the scaling curve. Including additional adiabatic potentials or higher orbital angular momenta L moves the point to the right along the scaling curve until convergence is reached. This trend is most evident in the calculation of Ref. [15], where the partial results for $L_{max}=0,2$ can be compared with the fully converged result with $L_{max}=4$ (see Tables 2 and 3 in Ref. [15]).

Note that the most accurate points in Fig. 2 all lie systematically above the scaling curve by approximately the same amount. One can interpret this deviation as being due to effective range effects. These effects are included in potential models, but the effective range is set to zero in the renormalized zero-range model and in the effective field theory which were used to calculate the scaling curve. It should be possible to account for these differences quantitatively by taking into account effective range corrections [34,35,53]. Since $r_s/a \approx 0.07$, we expect that including the effective range corrections as a first-order perturbation would shift the scaling curve by a small amount, bringing it into better agreement with the calculated points.

We can take into account the effective range corrections to $B_3^{(0)}$ approximately if we assume that the deviation $\Delta B_3^{(0)}$ of the leading-order universality prediction from the calculated value comes almost entirely from a correction linear in r_s . The calculated result for one potential can then be used to estimate the effective range corrections for the others. Choosing $B_3^{(0)}$ for the HFD-B potential as the input and denoting the deviations of $B_3^{(0)}$ from the leading-order universality predictions by $\Delta B_3^{(0)}$, we can estimate the effective range corrections for any other potential by

$$\left(\frac{\Delta B_3^{(0)}}{B_2} \right)_{\text{pot}} = \left(\frac{\Delta B_3^{(0)}}{B_2} \right)_{\text{HFD-B}} \frac{(r_s/a_B)_{\text{pot}}}{(r_s/a_B)_{\text{HFD-B}}}. \quad (15)$$

Since the various ${}^4\text{He}$ potentials have similar values of r_s , the shift $\Delta B_3^{(0)}$ is almost the same for all the potentials. The resulting predictions for $B_3^{(0)}$ are shown in column 5 of Table II. The corresponding prediction using a and $B_3^{(1)}$ as the input are shown in column 8. The predictions are labeled NLO

in Table II because they are approximate universality predictions at “next-to-leading order” in r_s/a . For each of the HFDHE2, LM2M2, and TTY potentials, the two NLO predictions differ by less than 3%. They also differ from the calculated results in column 1 by less than 3%.

We can use the results in Table II to give universality predictions for $B_3^{(0)}$ for potentials other than HFD-B both at LO and NLO in the effective range. As our best estimate, we take the average of the two predictions obtained by using B_2 and a as the two-body input. We take the difference to be an estimate of the theoretical error. The universality predictions for the TTY potential are

$$\text{LO: } B_3^{(0)} = 138 \pm 17 \text{ mK} \quad (\text{TTY}),$$

$$\text{NLO: } B_3^{(0)} = 127 \pm 2 \text{ mK} \quad (\text{TTY}). \quad (16)$$

The calculated value in column 1 of Table II lies within the error bar for both predictions. Note that including effective range corrections decreases the size of the error bar by an order of magnitude.

The identification of the excited state of the ${}^4\text{He}$ trimer as an Efimov state is well established [3,13–15,23,28–30]. We now discuss the question of whether the ground state of the ${}^4\text{He}$ trimer should be identified as an Efimov state. The good agreement between the universality prediction for $B_3^{(0)}$ and the calculated value could be fortuitous. Some authors have used as the criterion for an Efimov state that a sufficiently large increase in the strength of the two-body potential should make it unstable to decay into an atom and a dimer. Increasing the strength of the two-body potential decreases the scattering length. This tends to move the vertical dashed line in Fig. 1 to the right. A sufficiently large shift in the vertical line will move it beyond the point where that branch of Efimov states terminates on the line corresponding to the dimer binding energy. According to this criterion, the excited state of the trimer is an Efimov state but the ground state is not. However, we argue that the criterion for an Efimov state should not be based on how its binding energy behaves under a large deformation of the strength of the two-body potential, but on how it behaves under arbitrary small deformations of the potential. If it is an Efimov state, any small deformation of the two-body potential will move its binding energy along the universal scaling curve in Fig. 2. The various model potentials for ${}^4\text{He}$ can be interpreted as deformations of the “true” ${}^4\text{He}$ potential. The fact that the binding energies for these potentials lie along the universal curve is a convincing evidence that the ground state of the ${}^4\text{He}$ trimer is an Efimov state.

If the true binding energy $B_3^{(1)}$ of the excited ${}^4\text{He}$ trimer was measured and found to disagree with the calculated value using modern potentials, it would indicate that those potentials are not sufficiently accurate to predict low-energy three-body observables. Using the universality approach, there would be no need to improve the potential in order to predict these observables. We could simply take the measured value of $B_3^{(1)}$ as the input required to determine Λ_* . If we did choose to improve the potential, universality implies that to get predictions for low-energy three-body observables

TABLE III. The atom-dimer scattering lengths a_{12} and effective ranges $r_{s,12}$ in angstroms for four ^4He potentials. The calculated values of a_{12} from Ref. [15] are in column 1. The values of $a\Lambda_*$, the universality predictions for a_{12} , the predictions for a_{12} including effective range corrections, and the universality predictions for $r_{s,12}$ using B_2 and $B_3^{(1)}$ as input are in columns 2–5. The corresponding predictions using a and $B_3^{(1)}$ as input are in columns 6–9. Numbers in brackets were used as input.

Potential	a_{12}	$a_B\Lambda_*$	a_{12} (LO)	a_{12} (NLO)	$r_{s,12}$ (LO)	$a\Lambda_*$	a_{12} (LO)	a_{12} (NLO)	$r_{s,12}$ (LO)
HFDHE2	–	1.258	87.9	103(5)	278	1.364	65.8	101(5)	902
HFD-B	135(5)	0.922	120.2	[135(5)]	6.4	1.051	100.4	[135(5)]	18.6
LM2M2	131(5)	1.033	113.1	128(5)	16.0	1.155	92.8	128(5)	75
TTY	131(5)	1.025	114.5	129(5)	14.4	1.147	94.0	129(5)	69

with errors of order r_s/a , it would be sufficient to introduce a two-parameter deformation of the short-distance part of the potential and tune both parameters simultaneously so that the potential gives the correct values for B_2 and $B_3^{(1)}$. Alternatively, we could leave the two-body potential unchanged, but instead introduce an artificial short-range three-body potential and tune its strength in order to get the correct value for $B_3^{(1)}$. This is essentially what is done in the effective field theory approach; the parameter Λ_* is varied by adjusting the strength of a three-body contact interaction [3]. In the case of ^4He atoms, the “true” three-body potential decreases the binding energy $B_3^{(0)}$ of the ground-state trimer by about 0.3 mK [16]. Its effect on $B_3^{(1)}$ should be much smaller because the excited state is much larger in size. Thus, the effects of the “true” three-body potential on low-energy three-body observables should be very small. However, universality implies that the dominant effect on low-energy three-body observables from a deformation of the two-body potential that leaves the scattering length fixed is equivalent to the effect of adding a three-body potential.

IV. ATOM-DIMER SCATTERING

The differential cross section for the elastic scattering of an atom and a dimer with wave numbers k in the center-of-mass frame has the form

$$\frac{d\sigma}{d\Omega} = \left| \sum_{L=0}^{\infty} \frac{2L+1}{k \cot \delta_L(k) - ik} P_L(\cos \theta) \right|^2, \quad (17)$$

where $\delta_L(k)$ is the phase shift for the L^{th} partial wave. These phase shifts are real valued below the dimer breakup threshold at $k = (4mB_2/3\hbar^2)^{1/2}$. Above that threshold, they become complex valued because of the inelasticity from scattering into three-atom final states.

If the two-body scattering length is large, the cross section for low energies $E \lesssim \hbar^2/ma^2$ has a universal form. For $L \geq 1$, the phase shifts $\delta_L(k)$ are universal functions of ka only. To the best of our knowledge, they have not been calculated. The $L=0$ phase shift $\delta_0(k)$ is also universal, but it depends on $a\Lambda_*$ as well as on ka . The general structure of the dependence on $a\Lambda_*$ was deduced by Efimov [2]. For k below the breakup threshold, $ka \cot \delta_0$ can be written as

$$ka \cot \delta_0 = c_1(ka) + c_2(ka) \cot[s_0 \ln(a\Lambda_*) + \phi(ka)],$$

$$0 \leq ka \leq \frac{2}{\sqrt{3}}, \quad (18)$$

where $c_1(ka)$, $c_2(ka)$, and $\phi(ka)$ are unknown universal functions that satisfy the constraints $c_1(2/\sqrt{3})=0$ and $c_2(2/\sqrt{3})=2/\sqrt{3}$ [36]. Using the effective field theory of Ref. [3], we have calculated these functions. The results can be parametrized as follows:

$$c_1(ka) = -0.22 + 0.39k^2a^2 - 0.17k^4a^4,$$

$$c_2(ka) = 0.32 + 0.82k^2a^2 - 0.14k^4a^4,$$

$$\phi(ka) = 2.64 - 0.83k^2a^2 + 0.23k^4a^4. \quad (19)$$

The atom-dimer scattering length a_{12} and effective range $r_{s,12}$ are defined by the low-energy limit of the S -wave phase shift by an equation analogous to Eq. (2). From Eqs. (18) and (19), we obtain after the use of trigonometric identities

$$a_{12} = a(1.46 - 2.15 \tan[s_0 \ln(a\Lambda_*) + 0.09]), \quad (20)$$

$$r_{s,12} = a(1.30 - 1.64 \tan[s_0 \ln(a\Lambda_*) + 1.07] + 0.53 \tan^2[s_0 \ln(a\Lambda_*) + 1.07]). \quad (21)$$

The atom-dimer scattering lengths a_{12} for the HFD-B, LM2M2, and TTY potentials were calculated in Ref. [15], and the results are given in column 1 of Table III. Using the values of Λ_* determined in the preceding section, we can predict the atom-dimer scattering length and compare with the calculated values. The leading-order universality predictions for a_{12} and $r_{s,12}$ are given in columns 3, 5, 7, and 9 of Table III. If B_2 and $B_3^{(1)}$ are used as inputs, the predictions for a_{12} are smaller than the calculated values by about 13%. If a and $B_3^{(1)}$ are used as inputs, the predictions are smaller than the calculated values by about 28%. Note that the predictions for $r_{s,12}$ differ by as much as a factor of 5 depending on whether B_2 or a is used as the two-body input. In Fig. 3, we show the atom-dimer scattering parameters a_{12} and $r_{s,12}$ as functions of $a\Lambda_*$. The values of $a_B\Lambda_*$ and $a\Lambda_*$ for the TTY potential are indicated by the vertical dashed and dot-dashed lines, respectively. Note that $r_{s,12}$ is positive definite. It achieves a minimum value that is very close to zero near $a\Lambda_* = 0.94$ and diverges at $a\Lambda_* = 1.64$. The extracted values of $a\Lambda_*$ for ^4He are fortuitously in the interval between

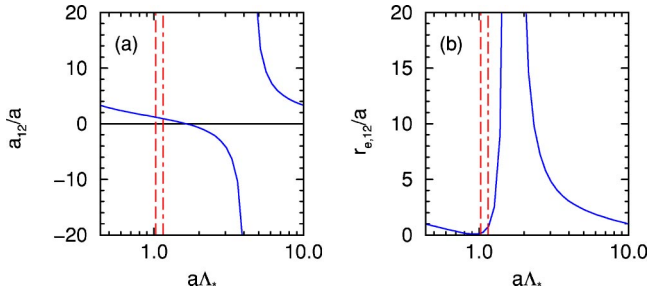


FIG. 3. The atom-dimer scattering length a_{12}/a (a) and effective range $r_{s,12}/a$ (b) as a function of $a\Lambda_*$. The values of $a_B\Lambda_*$ and $a\Lambda_*$ for the TTY potential are indicated by the vertical dashed and dot-dashed lines, respectively.

the minimum and the divergence where the effective range changes rapidly with $a\Lambda_*$. This leads to a large difference in the values of $r_{s,12}$ obtained from using a or B_2 as the two-body input.

In Fig. 4, we show the S -wave scattering phase shift $\delta_0(k)$ for the TTY potential as a function of the center-of-mass energy E_{cm} shifted by the dimer binding energy so that the scattering threshold is at zero energy,

$$E_{cm} + B_2 = \frac{3\hbar^2 k^2}{4m}, \quad (22)$$

where k is the wave number of the atom or the dimer. This shifted energy variable has the advantage that the position of the scattering threshold is independent of whether B_2 or a is taken as the two-body input. The solid and dashed lines show the universality prediction with B_2 and a as the two-body input, respectively. The vertical dashed and dot-dashed lines indicate the dimer breakup threshold for B_2 and a as the two-body input, respectively. The filled circles show the results of Ref. [15], which were obtained by solving the Faddeev equation with hard-core boundary conditions. The results are in good agreement with the error band defined by the solid and dashed curves.

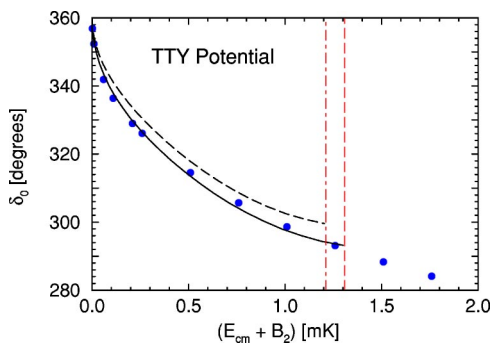


FIG. 4. The S -wave scattering phase shifts δ_0 for the TTY potential using B_2 as the two-body input (solid line) and using a as the two-body input (dashed line) as a function of the center-of-mass energy (with the scattering threshold defined as zero energy). The filled circles show the fully converged calculation of Ref. [15] with $L_{max}=4$. The vertical dashed and dot-dashed lines indicate the dimer breakup threshold for B_2 and a as the two-body input, respectively.

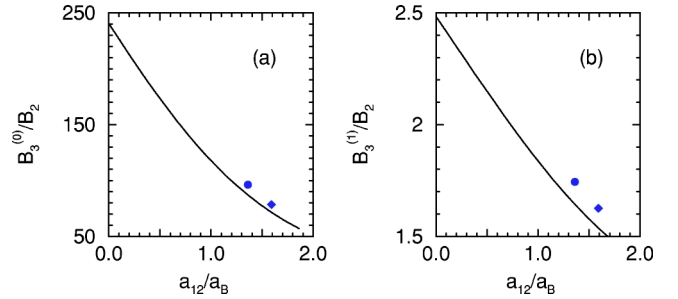


FIG. 5. The Phillips line for (a) the trimer ground state and (b) excited state. The solid line gives the universality prediction, while the data points show the results of Ref. [15] for the HFD-B (diamonds) and LM2M2/TTY potentials (circles).

Universality implies that the scaling variable a_{12}/a_B is a universal function of $a\Lambda_*$. By eliminating Λ_* , we can express $B_3^{(n)}/B_2$ as a universal function of a_{12}/a_B . The various ^4He potentials should all give binding energies and scattering lengths that lie along this curve. In nuclear physics, a similar correlation has been observed between the spin-doublet neutron-deuteron scattering length a_{12} and the binding energy of the triton B_3 and a_{12} using various potential models for the nucleon-nucleon interaction give results that cluster along a line in the a_{12} - B_3 plane called the Phillips line [37]. The observed values of B_3 and a_{12} also lie on that line. Modern nucleon-nucleon potentials predict a value for B_3 , which is about 5–10% below the measured value. Accurate values for both a_{12} and B_3 are obtained by adding a short-range three-body potential and adjusting one parameter to reproduce the measured triton binding energy. The Phillips line in nuclear physics arises from the large S -wave scattering length in both the spin-triplet ($r_s/a \approx 1/3$) and spin-singlet ($r_s/|a| \approx 1/8$) nucleon-nucleon channels [38,39,54]. In the case of ^4He , there are two Phillips lines: one for the ^4He trimer ground state and one for the excited state. These Phillips lines are shown in Figs. 5(a) and 5(b), respectively. The solid line is the universality prediction from Eqs. (10) and (20). As Λ_* increases, one moves along the solid line to the left. The data points show the results of Ref. [15] for the LM2M2/TTY (circles) and HFD-B potentials (diamonds). They lie close to the Phillips lines as expected from universality. For both potentials, the points lie slightly above the scaling curves, consistent with small effective range corrections.

We can use the calculated result for a_{12} for the HFD-B potential from Ref. [15] to estimate the effective range corrections for the other potentials. Denoting the deviation of a_{12} from the universality prediction by Δa_{12} , we can estimate the effective range correction by

$$\left(\frac{\Delta a_{12}}{a_B}\right)_{\text{pot}} = \left(\frac{\Delta a_{12}}{a_B}\right)_{\text{TTY}} \frac{(r_s/a_B)_{\text{pot}}}{(r_s/a_B)_{\text{TTY}}}. \quad (23)$$

The resulting predictions for a_{12} are shown in column 4 of Table III. The corresponding predictions using a and $B_3^{(1)}$ as the input are shown in column 8. The two NLO predictions

agree to within 2%. For the LM2M2 and TTY potentials, they agree with the calculated results in column 1 to within the error bars.

We can use the results in Table III to give universality predictions for potentials other than HFD-B for a_{12} both at leading order and next-to-leading order in the effective range. As the prediction and the theoretical error in a_{12} , we take the average and the difference of the predictions obtained by using B_2 and a as the two-body input. The universality predictions for the TTY potential are

$$\begin{aligned} \text{LO: } a_{12} &= (104 \pm 21) \text{ \AA} \quad (\text{TTY}), \\ \text{NLO: } a_{12} &= (129 \pm 5) \text{ \AA} \quad (\text{TTY}). \end{aligned} \quad (24)$$

The LO and NLO predictions for the TTY potential both agree to within errors with the calculated value in Table III. Including the effective range corrections decreases the error by about an order of magnitude. The error in the NLO prediction in Eq. (24) is dominated by the error in the calculated value for the HFD-B potential. There is no accurate calculation for $r_{s,12}$ for any of the ^4He potentials. Thus, we can only give a leading-order universality prediction for $r_{s,12}$. Since $r_{s,12}$ is positive definite and because it is so sensitive to the precise value of $a\Lambda_*$, we take the universality prediction for $r_{s,12}$ to be the geometric mean of the predictions obtained by using either B_2 or a as input. We take the theoretical uncertainty to be a multiplicative factor equal to the ratio of the two predictions. The resulting leading-order universality prediction for the TTY potential is then

$$\text{LO: } r_{s,12} = (32^{+121}_{-25}) \text{ \AA} \quad (\text{TTY}). \quad (25)$$

In spite of the large error bars, we can predict with confidence that $r_{s,12}$ is positive because the expression (21) is positive definite.

V. THREE-BODY RECOMBINATION

Three-body recombination is the process in which two of the three incoming atoms form a dimer and the third atom recoils to balance energy and momentum. The rate of three-body recombination events per unit time and unit volume in a gas of cold atoms is proportional to the third power of the number density [18]: $\nu = \alpha n^3$. The recombination rate constant α is a complicated function of the momenta of the three incoming atoms. At threshold, all three momenta vanish and α reduces to a number. The total three-body recombination rate is the sum of the rates for all the dimers.

If the scattering length a is large and positive, there is a shallow dimer with $B_2 = \hbar^2/ma^2$. The rate constant α for recombination into the shallow dimer at threshold must be a universal function of $a\Lambda_*$. It was calculated in Ref. [21] using the effective field theory of Ref. [3]. The result can be parametrized as

$$\alpha = 67.1 \sin^2[s_0 \ln(a\Lambda_*) + 0.19] \frac{\hbar a^4}{m}. \quad (26)$$

TABLE IV. The three-body recombination constant at threshold α in $10^{-27} \text{ cm}^6/\text{s}$. The leading order predictions from universality using B_2 and $B_3^{(1)}$ (a and $B_3^{(1)}$) as input are in column 2 (4). The corresponding values of $a\Lambda_*$ are given in column 1 (3).

Potential	$a_B\Lambda_*$	α (LO)	$a\Lambda_*$	α (LO)
HFDHE2	1.258	3.79	1.363	5.95
HFD-B	0.922	0.064	1.051	0.37
LM2M2	1.033	0.45	1.155	1.16
TTY	1.025	0.41	1.147	1.11

This remarkable oscillatory dependence on $\ln(a\Lambda_*)$ was previously observed in calculations using the hidden crossing theory [19] and the adiabatic hyperspherical representation [20]. In the hyperspherical representation, the oscillatory behavior arises from interference between two pathways from the incoming channel on the second adiabatic potential to the outgoing channel on the first adiabatic potential. Effective field theory allows the argument of the \sin^2 to be determined in terms of the same three-body parameter Λ_* that enters atom-dimer scattering and the trimer binding energies.

Using the values of Λ_* determined in Sec. III, we can predict the three-body recombination constant α from Eq. (26). Our predictions for α for four ^4He potentials are given in Table IV. The predictions vary by more than a factor of 2 depending on whether we take B_2 or a as the two-body input. This large difference arises because the value of $a\Lambda_*$ for ^4He atoms is fortuitously close to the value near $a\Lambda_* = 0.83$ at which the \sin^2 factor in Eq. (26) vanishes. This is illustrated in Fig. 6, where α in units of $\hbar a^4/m$ is plotted as a function of $a\Lambda_*$. The vertical dashed and dot-dashed lines indicate the values of $a_B\Lambda_*$ and $a\Lambda_*$ for the TTY potential, respectively. If we use a as input instead of B_2 , the \sin^2 factor is larger by a factor of two. Since α is positive definite and because it is so sensitive to the precise value of $a\Lambda_*$, we take the universality prediction to be the geometric mean of the predictions obtained by using either B_2 or a as the input. We take the theoretical uncertainty to be a multiplicative factor equal to the ratio of the two predictions. The resulting leading-order universality prediction for the TTY potential is

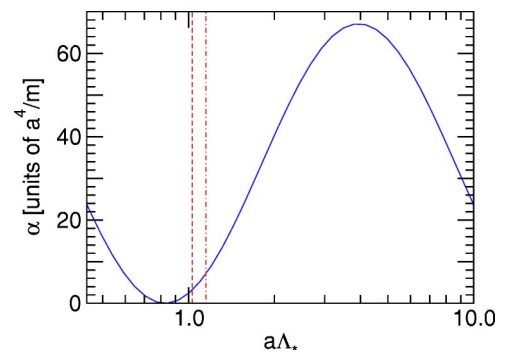


FIG. 6. The three-body recombination constant at threshold α in units of $\hbar a^4/m$ as a function of $a\Lambda_*$ (solid line). The values of $a_B\Lambda_*$ and $a\Lambda_*$ for the TTY potential are indicated by the vertical dashed and dot-dashed lines, respectively.

$$\text{LO: } \alpha = (0.7_{-0.4}^{+1.2}) \times 10^{-27} \text{ cm}^6/\text{s} \quad (\text{TTY}). \quad (27)$$

There have been several previous calculations of the three-body recombination rate at threshold for ^4He . Fedichev, Reynolds, and Shlyapnikov [18] calculated the rate by making a semianalytic approximation to the Faddeev equations in the hyperspherical representation. In the limit of large scattering length, they obtained a result that depends on a only: $\alpha = 3.9\hbar a^4/m$. They did not observe the oscillatory dependence of α on $\ln(a)$ predicted by Efimov theory, so there must have been an error in their analysis. They found that solving the Faddeev equations numerically for the TTY potential for ^4He gave corrections of about 10%. Inserting the value of a for the TTY potential into their analytical result, we obtain a prediction $\alpha = 0.6 \times 10^{-27} \text{ cm}^6/\text{s}$ that agrees with the universality prediction in Eq. (27). This agreement is probably fortuitous.

Nielsen and Macek [19] calculated the three-body recombination rate at threshold by applying hidden crossing theory to the Faddeev equations in the hyperspherical representation. They found that in the limit of large scattering length, α could take any value between 0 and $68\hbar a^4/m$ depending on some WKB phase. This is consistent with the effective field theory result in Eq. (26). For a Gaussian potential that gives the same scattering length and effective range as the LM2M2 potential, they obtained the prediction $\alpha = 1.1 \times 10^{-27} \text{ cm}^6/\text{s}$. They pointed out that the result is extremely sensitive to their WKB phase because it is close to the value for which α vanishes.

Esry, Greene, and Burke [20] calculated the three-body recombination rate at threshold by solving the Schrödinger equation in hyperspherical coordinates numerically for many potentials with one or at most a few two-body bound states. In the case $a > 0$, they found that the recombination rates could be well approximated by an empirical formula that reduces in the large a limit to an expression with an oscillatory dependence on $\ln a$ similar to Eq. (26). In the case of ^4He , their result for the HFD-B3-FCI1 potential [40] is $\alpha = 0.12 \times 10^{-27} \text{ cm}^6/\text{s}$. A new calculation in the hyperspherical adiabatic representation that also uses the HFD-B3-FCI1 potential has recently been carried out [22]. This calculation includes states with angular momentum $J > 0$, so that non-zero energies can be considered. At threshold, it agrees with the result of Ref. [20].

The large uncertainty in the universality prediction for α arises because the value of $a\Lambda_*$ for the ^4He potentials lies fortuitously close to the zero of Eq. (26). In order to improve on the universality prediction (26) within the effective field theory approach, it would be necessary to include effective range corrections. If there was an accurate calculation of α for a potential for which $B_3^{(1)}$ (or another low-energy three-body observable) is known, we could use that result to estimate the effective range corrections for other potentials. The only calculation of α we consider accurate enough is for the HFD-B3-FCI1 potential in Ref. [22]. Unfortunately, we are not aware of any calculation of $B_3^{(1)}$ for that potential.

VI. SUMMARY AND OUTLOOK

The universality approach to the three-body problem with large scattering length was pioneered by Efimov [2], who emphasized the qualitative insights it provides. This approach implies a correlation between all the low-energy three-body observables for potentials that have a large scattering length. The universality approach is also useful as a quantitative tool. It implies that up to corrections suppressed by l/a , all low-energy three-body observables are determined by a and a single three-body parameter. A convenient choice for the three-body parameter is the parameter Λ_* introduced in Ref. [3] because the dependence of some observables on Λ_* is known analytically.

In order to determine Λ_* , one three-body observable is required as input. A convenient choice is the binding energy of the shallowest Efimov state. Once Λ_* is determined, all other low-energy three-body observables can be predicted. We used calculations of the binding energy $B_3^{(1)}$ of the excited state of the trimer to determine Λ_* for various ^4He potentials. We then used universality to calculate the binding energy $B_3^{(0)}$ of the ground state of the trimer, the atom-dimer phase shifts below the dimer breakup threshold, and the three-body recombination constant at threshold α . We gave explicit expressions for the three-body recombination constant α in Eq. (26) and for the S -wave atom-dimer phase shifts below the breakup threshold in Eq. (18). We also gave an explicit parametrization for the universal function $\Delta(\xi)$ that appears in Efimov's equation (10) for the trimer binding energies.

The leading corrections to the universality predictions come from effective range corrections. If these corrections are included, there should be a systematic improvement in the accuracy of the predictions for all low-energy observables with errors decreasing to second order in l/a . The effective range corrections have not yet been calculated for the case of three identical spinless bosons with large scattering length. We therefore used accurate calculations of $B_3^{(0)}$ and a_{12} for the HFD-B potential as input to deduce the approximate effective range corrections in these observables for the other potentials. The resulting theoretical errors are smaller than those for the leading-order universality prediction by about an order of magnitude as expected. Comparing with the calculated values of $B_3^{(0)}$ and a_{12} , we see that the theoretical errors correctly reflect the accuracy of the LO and NLO universality predictions. An actual calculation of the effective range corrections for the three-body observables would eliminate the need for using calculations of three-body observables for one potential as additional inputs.

The leading-order universality predictions presented in this paper were obtained using the effective field theory of Ref. [3], which is a particularly convenient implementation of the universality approach for three-body systems. More generally, the effective field theory provides a framework for the model independent description of low-energy phenomena by exploiting a separation of scales in the system [41]. Using renormalization, all short-distance effects are systematically absorbed into a few low-energy parameters such as the scattering length a and Λ_* . As a consequence, the dependence

on the relevant low-energy parameters is explicit, while irrelevant details of how their numerical values arise from complicated short-distance dynamics are omitted. The effective field theory allows for systematically improvable calculations of low-energy observables with well-defined error estimates. This method has many applications ranging from particle physics over nuclear physics to condensed-matter physics [42–44].

An important open question is that how universality is manifested in the four-body problem. Low-energy four-body observables must depend on the two-body parameter a and the three-body parameter Λ_* . Are any new four-body parameters required to calculate low-energy four-body observables up to corrections suppressed by $l/|a|$? There are theoretical arguments in support of both answers to this question. There is a renormalization argument for zero-range δ -function two-body potentials that indicates that a new four-body parameter is required to calculate four-body binding energies [45]. On the other hand, a power counting argument within the effective field theory framework suggests that a four-body parameter should not be necessary to calculate four-body observables to leading order in $l/|a|$ [46]. This raises the exciting possibility of calculating the binding energy of the ${}^4\text{He}$ tetramers close to the four-atom threshold to about 10% accuracy using a and $B_3^{(1)}$ (or another low-energy three-body observable) as the only inputs. There is some circumstantial evidence in favor of this possibility from the four-body problem in nuclear physics. There is a correlation called the “Tjon line” between the binding energy B_3 of the triton (${}^3\text{H}$ nucleus) and the binding energy B_4 of the α particle (${}^4\text{He}$ nucleus) [47]. Calculations of these binding energies using modern nucleon-nucleon interaction potentials give results that underestimate both binding energies but cluster along a line in the B_3 - B_4 plane. By adding a three-body potential whose strength is adjusted to get the correct value for B_3 , one also gets an accurate result for B_4 (see Ref. [48] for some recent calculations with modern nuclear forces).

The results for ${}^4\text{He}$ presented in the paper apply equally well to other bosonic atoms with large scattering length as long as the effects of deep two-body bound states on low-energy observables are sufficiently small. By definition, a deep bound state has a binding energy of order \hbar^2/ml^2 or larger. If $a < 0$, any dimer is deeply bound. If $a > 0$, any dimer other than the shallow dimer with $B_2 \approx \hbar^2/ma^2$ is deeply bound. One qualitative effect of the deep two-body states is that the Efimov states become resonances because they can decay into an atom and a deeply bound dimer. Deep two-body bound states also provide additional channels for three-body recombination. Their effects can be particularly dramatic for $a < 0$ if there is an Efimov state near the three-atom threshold because it gives a resonant enhancement of the three-body recombination rate into deep two-body bound states [20,49]. The existence of deep two-body bound states does not affect the universality prediction for low-energy observables in the two-body sector. However, in the three-body sector, it implies that a third parameter in addition to a and Λ_* is required to predict low-energy observables up to corrections suppressed by $l/|a|$ [49]. This parameter takes into

account the cumulative effects of all the deep two-body bound states. The modification of Efimov’s equation for the binding energies was given in Ref. [30].

The universality approach discussed in this paper is not limited to identical bosons. It can be applied to any three-particle system for which at least two of the three pairs have a large scattering length. Some examples are given in a recent review article [50]. The universality predictions will depend on the three pairwise scattering lengths, the ratios of the masses, and the three-body parameter Λ_* .

An especially promising application of the universality approach is to cold atoms in the vicinity of a Feshbach resonance, where the effective scattering length can be controlled by an external magnetic field [4]. This creates the exciting possibility of testing the unique oscillatory dependence of low-energy three-body observables on the scattering length that is predicted by universality. In this paper, we have exploited the fact that the various ${}^4\text{He}$ potentials span a small interval of $a\Lambda_*$. Using a Feshbach resonance to control the scattering length, it might be possible to scan through an entire cycle of the oscillatory behavior. Among the dramatic effects that one may be able to observe are the divergence in a_{12} near $a\Lambda_* = 4.3$ and the zero of α near $a\Lambda_* = 0.83$.

The behavior of cold atoms near a Feshbach resonance is in general a complicated coupled-channel problem involving the various hyperfine states of the atoms. However, from the point of view of universality, the coupled-channel effects introduce no additional complications. If one is sufficiently close to the resonance and if the energy relative to the threshold for one hyperfine state is small as compared to the hyperfine splittings, only that hyperfine state needs to be included explicitly. The coupled-channel effects can be taken into account through the values of the low-energy parameters a , which diverges at the resonance, and Λ_* , which varies slowly in the neighborhood of the resonance.

The behavior of a Bose-Einstein condensate of atoms with large scattering lengths has been studied experimentally by using Feshbach resonances to tune the scattering lengths of alkali atoms [6]. In the low-density limit $na^3 \ll 1$, the non-trivial aspects of universality in the three-body sector are reflected in a small oscillatory dependence of the energy density of the condensate on $\ln(\Lambda_* n^{1/3})$ [51]. There is a possibility that these three-body effects would allow the existence of stable homogeneous condensates with large negative scattering length [52]. The intermediate density region, where $na^3 \sim 1$ but $nl^3 \ll 1$ is a more difficult problem. It is an open question whether or not a condensate in this region has universal properties that are determined by constants such as a and Λ_* that describe the low-energy properties in the few-body sectors. If there are, it may be possible to use universality to predict in detail the behavior of a Bose-Einstein condensate of atoms near a Feshbach resonance.

ACKNOWLEDGMENTS

We thank D. Blume, B.D. Esry, and C.H. Greene for useful correspondence. This research was supported by Department of Energy Grant No. DE-FG02-91-ER4069 and NSF Grant No. PHY-0098645.

- [1] L.D. Landau and E.M. Lifshitz, *Quantum Mechanics: Nonrelativistic Theory* (Pergamon, New York, 1965); J.J. Sakurai, *Modern Quantum Mechanics* (Addison-Wesley, Reading, MA, 1985).
- [2] V.N. Efimov, *Yad. Fiz.* **12**, 1080 (1970) [*Sov. J. Nucl. Phys.* **12**, 589 (1971)]; **29**, 1081 (1979); [**29**, 546 (1979)]; *Nucl. Phys. A* **210**, 157 (1973).
- [3] P.F. Bedaque, H.-W. Hammer, and U. van Kolck, *Phys. Rev. Lett.* **82**, 463 (1999); *Nucl. Phys. A* **646**, 444 (1999).
- [4] E. Tiesinga, B.J. Verhaar, and H.T.C. Stoof, *Phys. Rev. A* **47**, 4114 (1993); A.J. Moerdijk, B.J. Verhaar, and A. Axelsson, *ibid.* **51**, 4852 (1995).
- [5] E. Nielsen, D.V. Fedorov, and A.S. Jensen, *Phys. Rev. Lett.* **82**, 2844 (1999).
- [6] S. Inouye *et al.*, *Nature (London)* **392**, 151 (1998); P. Courteille *et al.*, *Phys. Rev. Lett.* **81**, 69 (1998); S.L. Cornish *et al.*, *ibid.* **85**, 1795 (2000); N.R. Claussen *et al.*, e-print cond-mat/0201400.
- [7] R.E. Grisenti *et al.*, *Phys. Rev. Lett.* **85**, 2284 (2000).
- [8] A.R. Janzen and R.A. Aziz, *J. Chem. Phys.* **103**, 9626 (1995).
- [9] W. Schöllkopf and J.P. Toennies, *J. Chem. Phys.* **104**, 1155 (1996).
- [10] L.W. Bruch, W. Schöllkopf, and J.P. Toennies, *J. Chem. Phys.* **117**, 1544 (2002).
- [11] R.A. Aziz and M.J. Slaman, *J. Chem. Phys.* **94**, 8047 (1991).
- [12] K.T. Tang, J.P. Toennies, and C.L. Yiu, *Phys. Rev. Lett.* **74**, 1546 (1995).
- [13] E. Nielsen, D.V. Fedorov, and A.S. Jensen, *J. Phys. B* **31**, 4085 (1998).
- [14] V. Roudnev and S. Yakovlev, *Chem. Phys. Lett.* **328**, 97 (2000).
- [15] A.K. Motovilov, W. Sandhas, S.A. Sofianos, and E.A. Kolganova, *Eur. Phys. J. B* **13**, 33 (2001).
- [16] M. Lewerenz, *J. Chem. Phys.* **106**, 4596 (1997).
- [17] D. Blume and C.H. Greene, *J. Chem. Phys.* **112**, 8053 (2000).
- [18] P.O. Fedichev, M.W. Reynolds, and G.V. Shlyapnikov, *Phys. Rev. Lett.* **77**, 2921 (1996).
- [19] E. Nielsen and J.H. Macek, *Phys. Rev. Lett.* **83**, 1566 (1999).
- [20] B.D. Esry, C.H. Greene, and J.P. Burke, *Phys. Rev. Lett.* **83**, 1751 (1999).
- [21] P.F. Bedaque, E. Braaten, and H.-W. Hammer, *Phys. Rev. Lett.* **85**, 908 (2000).
- [22] H. Suno, B.D. Esry, C.H. Greene, and J.P. Burke, *Phys. Rev. A* **65**, 042725 (2002).
- [23] T. Frederico, L. Tomio, A. Delfino, and A.E.A. Amorim, *Phys. Rev. A* **60**, R9 (1999).
- [24] A. Delfino, T. Frederico, and L. Tomio, *Few-Body Syst.* **28**, 259 (2000).
- [25] G.F. Gribakin and V.V. Flambaum, *Phys. Rev. A* **48**, 546 (1993); B. Gao, *ibid.* **58**, 4222 (1993); V.V. Flambaum, G.F. Gribakin, and C. Harabati, *ibid.* **59**, 1998 (1999); C. Boisseau, E. Audouard, J. Vigue, and V.V. Flambaum, *Eur. Phys. J. D* **12**, 199 (2000).
- [26] R.A. Aziz *et al.*, *J. Chem. Phys.* **70**, 4330 (1979).
- [27] R.A. Aziz, F.R.W. Court, and C.C.K. Wong, *Mol. Phys.* **61**, 1487 (1987).
- [28] T.K. Lim, S.K. Duffy, and W.C. Damert, *Phys. Rev. Lett.* **38**, 341 (1977).
- [29] B.D. Esry, C.D. Lin, and C.H. Greene, *Phys. Rev. A* **54**, 394 (1996).
- [30] E. Braaten, H.-W. Hammer, and M. Kusunoki, *Phys. Rev. A* (to be published), e-print cond-mat/0201281.
- [31] Th. Cornelius and W. Glöckle, *J. Chem. Phys.* **85**, 3906 (1986).
- [32] T. González-Lezana *et al.*, *Phys. Rev. Lett.* **82**, 1648 (1999).
- [33] B.D. Esry *et al.*, *Phys. Rev. Lett.* **86**, 4189 (2001).
- [34] V. Efimov, *Phys. Rev. C* **44**, 2303 (1991); **47**, 1876 (1993).
- [35] H.-W. Hammer and T. Mehen, *Phys. Lett. B* **516**, 353 (2001).
- [36] E. Braaten and H.-W. Hammer (unpublished).
- [37] A.C. Phillips, *Nucl. Phys. A* **107**, 209 (1968).
- [38] V. Efimov and E.G. Tkachenko, *Yad. Fiz.* **47**, 29 (1988) [*Sov. J. Nucl. Phys.* **47**, 17 (1988)]; *Few-Body Syst.* **4**, 71 (1988).
- [39] P.F. Bedaque, H.-W. Hammer, and U. van Kolck, *Nucl. Phys. A* **676**, 357 (2000).
- [40] R.A. Aziz, A.R. Janzen, and M.R. Moldover, *Phys. Rev. Lett.* **74**, 1586 (1995).
- [41] G.P. Lepage, in *From Actions to Answers, TASI'89*, edited by T. DeGrand and D. Toussaint (World Scientific, Singapore, 1990); G.P. Lepage, e-print nucl-th/9706029; D.B. Kaplan, e-print nucl-th/9506035.
- [42] H. Georgi, *Annu. Rev. Nucl. Part. Sci.* **43**, 209 (1993); A.V. Manohar, e-print hep-ph/9606222.
- [43] U. van Kolck, *Prog. Part. Nucl. Phys.* **43**, 337 (1999); S.R. Beane *et al.*, e-print nucl-th/0008064.
- [44] R. Shankar, e-print cond-mat/9703210; J. Polchinski, e-print hep-th/9210046; H. Leutwyler, hep-ph/9609466; C.P. Hofmann, e-print cond-mat/9805277.
- [45] S.K. Adhikari, T. Frederico, and I.D. Goldman, *Phys. Rev. Lett.* **74**, 487 (1995).
- [46] G.P. Lepage (private communication).
- [47] J.A. Tjon, *Phys. Lett. B* **56**, 217 (1975).
- [48] A. Nogga, H. Kamada, and W. Glöckle, *Phys. Rev. Lett.* **85**, 944 (2000).
- [49] E. Braaten and H.-W. Hammer, *Phys. Rev. Lett.* **87**, 160407 (2001).
- [50] E. Nielsen, D.V. Fedorov, A.S. Jensen, and E. Garrido, *Phys. Rep.* **347**, 373 (2001).
- [51] E. Braaten, H.-W. Hammer, and T. Mehen, *Phys. Rev. Lett.* **88**, 040401 (2002).
- [52] A. Bulgac, *Phys. Rev. Lett.* **89**, 050402 (2002).
- [53] The short-range part of the “true” potential can be defined by the leading-order Born-Oppenheimer approximation. Corrections to this approximation are suppressed by m_e/m , where m_e is the electron mass.
- [54] The values of $K_3 = 6\alpha$ given in the “present” column of Table I in Ref. [20] must be divided by 6 in order to correct for a factor of 6 error in Eq. (1) of that paper.